



Observation and modelling of bubble dynamics in isolated bubble regime in subcooled flow boiling



Tomio Okawa*, Kazuhiro Kaiho, Shintaro Sakamoto, Koji Enoki

Department of Mechanical and Intelligent Systems Engineering, The University of Electro-Communications, 1-5-1, Chofugaoka, Chofu-shi, Tokyo 182-8585, Japan

ARTICLE INFO

Keywords:

Subcooled flow boiling
Bubble dynamics
Lift-off
Visualization
Lagrangian simulation

ABSTRACT

Experiments of subcooled flow boiling in isolated bubble regime were conducted to understand the dynamics of individual bubbles. The test fluid was water, the flow direction was vertical upward, and the pressure was slightly higher than the atmospheric pressure. In the present experiments, the bubbles produced at nucleation sites were commonly lifted off the vertical heated surface. They were then propelled into the subcooled bulk liquid to disappear due to heat transfer with subcooled liquid. It was frequently observed that the bubbles were suddenly accelerated in the lateral direction before the disappearance. Using the present observation results, new correlations were developed for the bubble lift-off velocity and the bubble acceleration phenomenon after the lift-off. It was shown that the bubble trajectories and the time-variation of bubble size calculated using the present correlations are in fairly good agreement with the experimental results.

1. Introduction

Accurate prediction of the void fraction in subcooled boiling region is of considerable importance in the field of nuclear engineering since it influences the core flow rate, the onset of two-phase flow instability, and the fuel burnup in light water reactors. In the numerical simulation of subcooled flow boiling, empirical methods are usually used (Levy, 1967; Saha and Zuber, 1974; Lahey, 1978), but reliability of empirical methods are deteriorated if they are applied to the thermal-hydraulic conditions in which no experimental data is available. Thus, in recent years, various mechanistic subcooled flow boiling models have been developed to reduce the uncertainty of numerical results (Kurul and Podowski, 1990; Basu et al., 2005; Kljenak and Mavko, 2006; Yeoh et al., 2008).

In water subcooled flow boiling at low pressure, bubbles were usually lifted off the heated surface immediately after the nucleation at nucleation sites (Prodanovic et al., 2002; Situ et al., 2005; Bibeau and Salcudean, 1994; Okawa et al., 2005; Ahmadi et al., 2012; Kaiho et al., 2017). If the lateral bubble velocity at the lift-off is high, the bubble moves from the superheated liquid region near the heated wall to the low-temperature bulk liquid within a short time. In addition, the heat transfer coefficient should also be high since the bubble velocity relative to the liquid increases. In consequence, the bubble life time is considered to be shortened if the bubble velocity at lift-off is high since the condensation of the bubble is enhanced. It is therefore considered that the bubble velocity at the instant of lift-off from the heated surface

is of importance in predicting the void fraction in subcooled boiling region accurately.

In mechanistic modeling of subcooled flow boiling, experimental information is needed for the bubble dynamics from various aspects. Thus, detailed visualization of bubbles produced in subcooled flow boiling has extensively been conducted (Prodanovic et al., 2002; Situ et al., 2005; Okawa et al., 2005; Ahmadi et al., 2012; Kaiho et al., 2017; Thornecroft et al., 1998). In these experiments, various bubble parameters including the bubble departure diameter, bubble lift-off diameter, nucleation site density, and bubble release frequency were measured. However, no systematic experimental information is available for the bubble lift-off velocity. In the present work, visualization of subcooled flow boiling is carried out in the isolated bubble regime to measure the bubble velocity components in the lateral and vertical directions at lift-off. In the experiments, it was observed that many bubbles were suddenly accelerated after several milliseconds from the lift-off. Based on these observation results, correlations are developed for the bubble lift-off velocity and the bubble acceleration phenomenon. Simple bubble tracking simulation is performed using the proposed correlations to show that the time-variation of bubble size and the bubble trajectory calculated using the present models are in fairly good agreement with the observation results.

* Corresponding author.

E-mail address: okawa.tomio@uec.ac.jp (T. Okawa).

Nomenclature

C_A	deformation parameter (dimensionless)
C_t	model constant (dimensionless)
C_u	model constant (dimensionless)
C_{VM}	virtual mass coefficient (dimensionless)
c_p	specific heat (J/kg·K)
D	hydraulic-equivalent channel diameter (m)
d	diameter (m)
f_{drag}	drag force (N/m ³)
f_{lift}	lift force (N/m ³)
f_{vm}	virtual mass force (N/m ³)
f_w	wall friction factor (dimensionless)
G	mass flux (kg/m ² s)
g	gravitational acceleration (m/s ²)
h_{end}	condensation heat transfer coefficient (W/m ² K)
Ja	Jacob number (dimensionless)
KE	kinetic energy (J)
l	Laplace length (m)
p	pressure (Pa)
q_w	heat flux (W/m ²)
R_A	aspect ratio (dimensionless)
Re	Reynolds number (dimensionless)
r	radius (m)
SE	surface energy (J)
t	time from nucleation (s)
u	velocity (m/s)
u	velocity in the lateral direction (m/s)
v	velocity in the vertical direction (m/s)

x	position (m)
x	distance from the wall (m)
y	vertical position from the nucleation site (m)

Greek symbols

α	thermal diffusivity (m ² /s)
Δh_v	latent heat of vaporization (J/kg)
ΔT_{sub}	subcooling (K)
ΔT_w	wall superheat (K)
Δu	velocity difference (K)
μ	viscosity (Pa·s)
θ	contact angle (rad)
ρ	density (kg/m ³)
σ	surface tension (N/m)

Superscripts

b	bubble center position
+	dimensionless

Subscripts

acc	acceleration
b	bubble
l	liquid phase
lift	lift-off
max	maximum
v	vapor phase

2. Experiments**2.1. Experimental apparatus**

Fig. 1 depicts the schematic diagram of the experimental loop. More detailed description of the experimental apparatus is found in Kaiho et al. (2017). First, filtrated and deionized tap water was supplied to the loop. The water was then circulated using a gear pump and the loop was kept at low pressure about 15 kPa for about 24 h using the vacuum pump for vacuum degassing. Then, the mass flux G was adjusted at the desired value using the flow control valves and the turbine flow meter.

Then, the preheater was used to set the inlet subcooling ΔT_{sub} . The fluid temperature and the pressure were measured at the inlet of the test section using the type-K thermocouple and pressure transducer. The measurement accuracy was within ± 1.2 kg/m²s for the mass flux, ± 2.5 K for the fluid temperature and ± 5 kPa for the pressure. After exiting the test section, the test fluid entered the separator tank that was open to atmosphere. The vapor phase was condensed or released to atmosphere whilst the liquid phase was returned to the circulation pump through the plate-type heat exchanger where the fluid temperature was reduced by the heat transfer with the cooling water.

The schematic diagram of the test section is delineated in Fig. 2. A

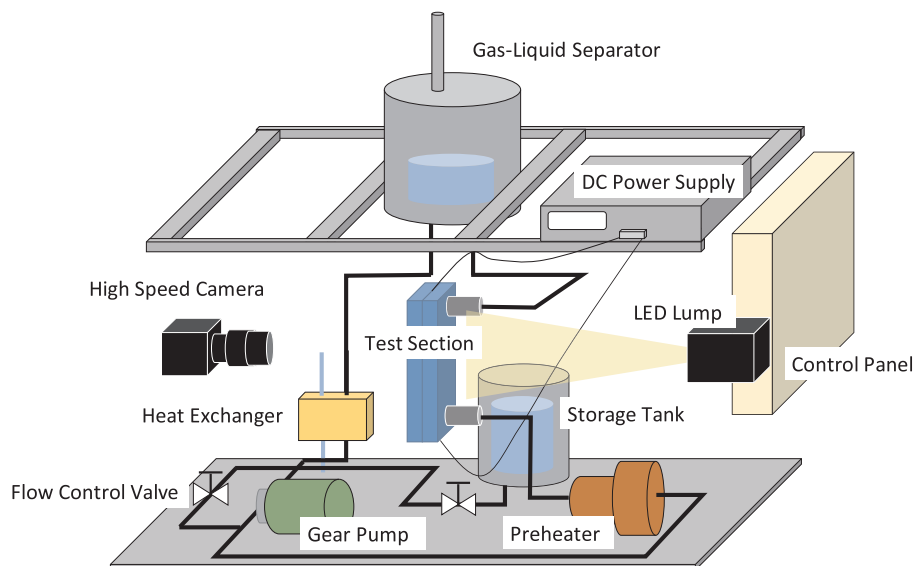


Fig. 1. Schematic diagram of the experimental loop.

Download English Version:

<https://daneshyari.com/en/article/6758839>

Download Persian Version:

<https://daneshyari.com/article/6758839>

[Daneshyari.com](https://daneshyari.com)